Albert-Ludwigs-Universität Freiburg
Advanced Physics Lab Course
Summer Semester 2022

Experiment on 05.-06.09.2022

Scanning tunnelling microscope

Group 13:
08.09.2022

Assistant:

Abstract

In the experiment “scanning tunnelling microscope“, the atomic structure of graphite, gold and MoS_2 should be examined by measuring the tunnelling current between the tip and the surface with a scanning tunnelling microscope. From the measured surface structure one can calculate the lattice constant of the respective sample.

The measurement of the graphite lead to very noisy and blurry surface structures that couldn't be analysed properly. As a consequence the measurements of gold and MoS_2 couldn't be performed at all. Therefore a very detailed discussion section analysing the main problems and possible improvements is added.

Contents

List of Tables

List of Figures

1 Introduction

In this experiment the surface structures – and therefore the lattice constants – of different samples are studied by measuring the surface with a scanning tunnelling microscope. As the first part of the experiment focuses on measuring the structure and calculating the lattice constant of graphite and thereby assessing the quality of the produced tip, the second part mainly studies the surface structure of gold, which isn't expected to be resolvable on atomic level.
The third part, in which the measurement is performed on the MoS_2, also focuses on the surface structure and the lattice constant. Due to MoS_2 being a semi-conductor one can evaluate two different structures by applying differently orientated voltages between the sample and the measuring tip.

2 Theory of scanning tunnelling microscopy

The following sections introducing the theory necessary for the experiment are mainly based on the experiment description, which is provided by the advanced physics lab team [1] and the diploma thesis by Dieter Ritzmann [2]. For subsection 2.3 about the quantum tunnelling effect the script of the theoretical physics III lecture by Prof. Dr. Gerhard Stock [3] is also used.

2.1 Table of the used variables

Tab. 1: Table of the used symbols for the parameters used in the protocol. The upper part lists the symbols used in the theory section, whereas the lower part of the table introduces the symbols for the analysis part.

Symbol	Parameter
$\Psi(x)$	wave function
E	energy of a quantum object
E_F	Fermi-energy
m	mass of a quantum object
$\hbar$	reduced Planck constant
V, V_0	potential, potential of the barrier
Φ	effective barrier height
L	length of the barrier
T	transmission
I	tunnelling current
U	applied voltage
ρ	local states density
R	radius of the tip
d	lattice constant
l	distance between two maxima
m	number of minima between maxima

2.2 Electronic band structure

In the solid state physics, a crystal with a periodic structure and its energy levels can be described with the electronic band model [4]. In this model the energy states are structured in bands of almost continuous energy states with gaps between them. The energy that indicates the border of filled and empty energy states in the ground state is called the Fermi-Energy E_F [4]. If the Fermi-Energy lays inside a bond, the material is a conductor, because electrons can easily flow

due to plenty of free energy states next to their states. In isolators and semi-conductors, the Fermi-Energy lays in a gap between conduction band and valance band [4]. In Figure 1 the energy bonds of an isolator and two different conductors together with the Fermi-Energy E_F are presented.

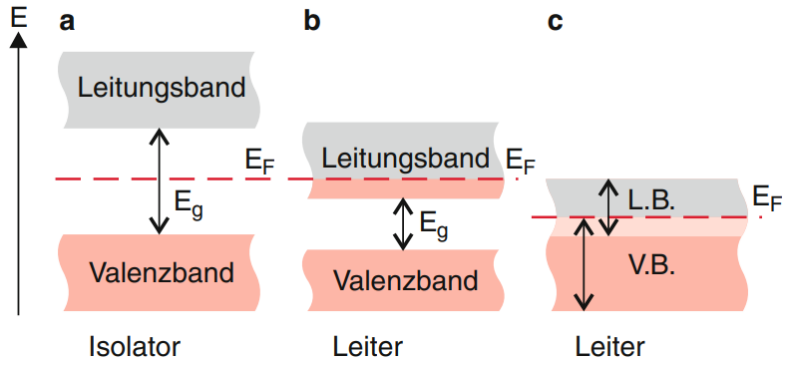

Fig. 1: In this graphic one can see the electronic band structure of an isolator on the left and two conductors on the right. In addition the Fermi-Energy E_F and the energy gap E_g between conduction band (grey) and valance band (red) is illustrated. This graphic is taken from [4].

2.3 Quantum tunnelling

The fundamental theory for the experiment is the quantum tunnelling effect, where an object with a smaller energy can „tunnel“ through a classically forbidden area with a higher potential. The potential barrier with the length L can be described with the following potential [3]:

$$V(x) = \begin{cases} 0 & x < 0 \\ V_0 & 0 \leq x \leq L \\ 0 & x > L. \end{cases} \tag{1}$$

This potential and the energy of the quantum object E, which is smaller than V_0, are portrayed in Figure 2.

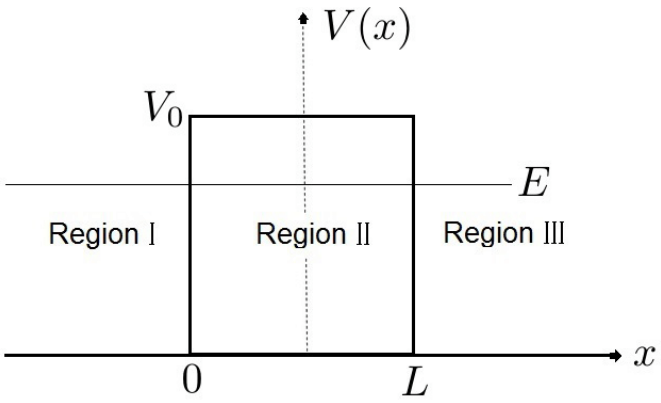

Fig. 2: Sketch of the potential barrier with the height V_0 and the length L and the smaller energy E of the quantum object. This graphic is taken from [5].

As an approach to find a wave function for this problem one can choose [3]:

$$\Psi(x) = \begin{cases} e^{ik_0 x} + \rho e^{-ik_0 x} & x < 0 \\ \alpha e^{ikx} + \beta e^{-ikx} & 0 \leq x \leq L \\ \tau e^{ik_0 x} & x > L, \end{cases} \tag{2}$$

$$k_0 = \sqrt{\frac{2mE}{\hbar^2}} \quad \text{and} \quad k = \sqrt{\frac{2m(E - V_0)}{\hbar^2}} \quad \text{and} \quad \alpha, \beta, \rho, \tau \in \mathbb{C}. \tag{3}$$

Therefore the probability of the object tunnelling the barrier is given as $T = |\tau|^2$ [3]. The parameters α, β, ρ and τ can be found by solving the continuity conditions of $\Psi(x)$ and $\Psi'(x)$ for $x = 0$ and $x = L$. This leads to [3]:

$$T = \frac{1}{1 + \gamma \sinh^2(\kappa L)}, \tag{4}$$

$$\gamma = \frac{1}{4}\left(\frac{k_0}{k} - \frac{k}{k_0}\right)^2, \tag{5}$$

$$\kappa = \sqrt{\frac{2m(V_0 - E)}{\hbar^2}}. \tag{6}$$

As a consequence the probability of the quantum object tunnelling the barrier is not zero and the resulting wave function can be found in Figure 3.

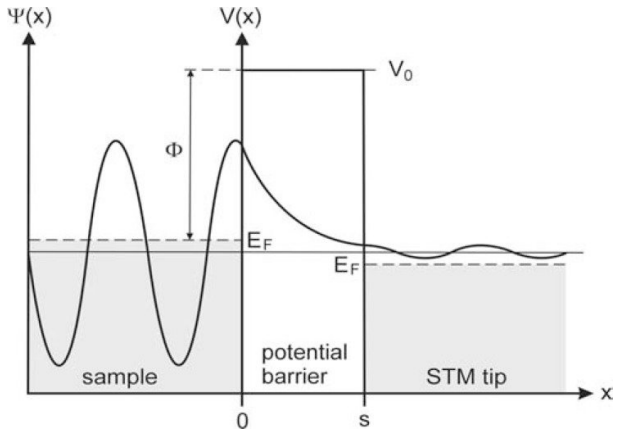

Fig. 3: In this graphic one can see the potential barrier from 0 to s with the height V_0 and the wave function of the quantum object. On the left side of the barrier one can also see the Fermi-energy E_F of the sample and on the right side of the STM tip. Both of those energies are lower than the potential barrier and the difference of the Fermi-energy E_F of the sample and V_0 is illustrated as Φ. This graphic is taken from [6].

2.4 Usage of quantum tunnelling for the scanning tunnelling microscope

For the experiment the quantum tunnelling effect can be used as a model for the potential between tip and sample. Because of quantum tunnelling, a current I between tip and sample can be measured, which is exponentially dependent on the distance L between tip and sample and Φ, which is the effective barrier height. It is also dependent on the voltage U applied between the tip and the sample [2]:

$$I \propto U e^{-\sqrt{\frac{2m\Phi}{\hbar}}L}. \tag{7}$$

With perturbation theory, one can find a proportionality between the current I of an ideal sharp tip and the local state density ρ [2]:

$$I \propto \sum_{\nu} |\Psi_\nu(\vec{r})|^2 \delta(E_\nu - E_F) = \rho(\vec{r}, E_F). \tag{8}$$

$\Psi_\nu(\vec{r})$ is the wave function of the state of energy E_ν and E_F is the Fermi-energy. Because it is not realistic to get a perfectly sharp tip, a correction term for a tip of radius R is needed [2]:

$$I \propto U e^{-2k(R+L)} \rho(\vec{r}, E_F). \tag{9}$$

With a scanning tunnelling microscope, the surface of a sample is scanned by measuring the tunnelling current and so the state density. As a result the structure of the surface can be examined. In general, there are two different modes for the microscope to scan the surface. In the constant current mode the tunnelling current is measured and by a feedback loop the distance of the tip is set to a constant level. Therefore the position of the tip is varied while the current is hold constant. In the constant height mode the height of the tip is held constant and the tunnelling current is measured to get the distance between tip and sample. In Figure 4 both modes are illustrated.

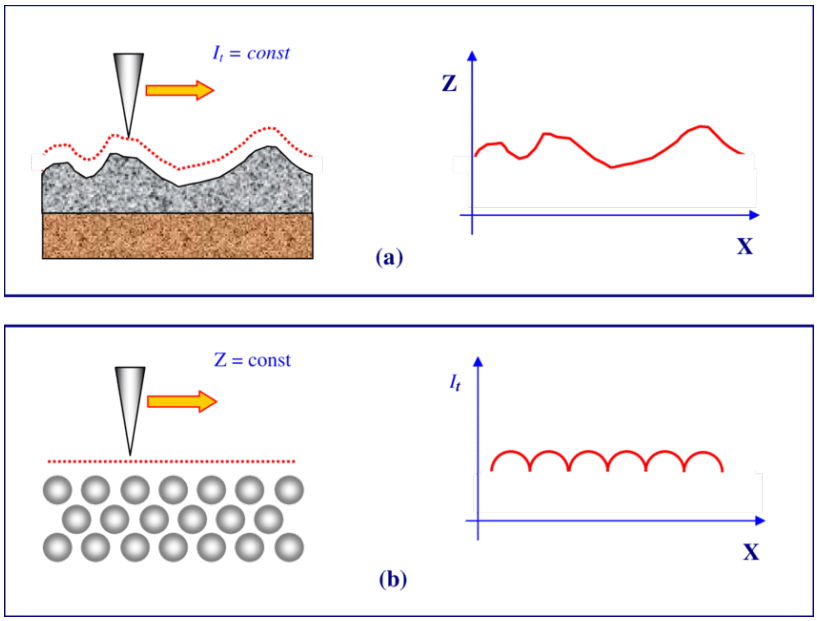

Fig. 4: In the top graphic one can see a tip measuring in the constant current mode and in the bottom graphic in the constant height mode. The graphic is taken from [7].

2.5 Characteristics of the used samples

In the first measurement we examine a graphite sample. Graphite is built out of hexagonal patterns in different layers. In α-atoms two layers have an atom at the same postion in the grid, which gives a stronger bond and therefore lower energy state. In contrast, β-atoms lay over gaps of the lower layer and have therefore a higher energy state. This leads to only β-atoms being visible by the microscope, because mostly the electrons with an energy closer to the Fermi-energy are tunnelling [2]. Therefore we get a more triangular pattern. The structure of graphite is visualised in Figure 5.

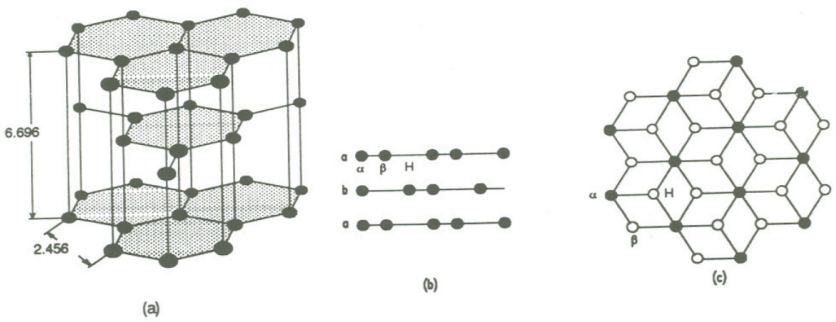

Fig. 5: In the left picture one can see three layers of graphite with all the distances being in Å. In the picture in the middle the difference in the α- and β-atoms are visualised. In the right picture the structure of the graphite can be seen from the top with the different atoms being marked. This graphic is taken from [2].

The second sample is gold, which is a metal. In a metal, one of the energy bonds is only partly filled with states so that electrons can travel through it. The electrons in the highest states can than tunnel through the potential barrier into the tip. Those electrons can be measured as the tunnelling current [2].

In a last step a MoS_2 is examined with the microscope. As a semi-conductor MoS_2 has a gap between valance and conduction band and electrons can only flow because of thermal energy or doping. In MoS_2, there are layers of molybdenum between two layers of sulphur. This structure can be seen in Figure 6.

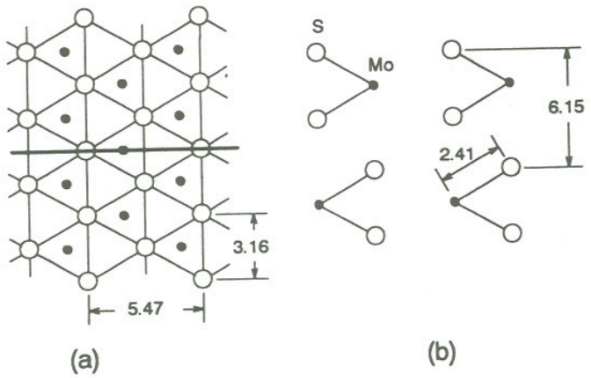

Fig. 6: In the left picture one can see the structure of the MoS_2 with all the distances being in Å. The black dots represent the molybdenum and the white dots show the sulphur. In the right picture other distances between the molybdenum and the sulphur are presented, which are again in Å. This graphic is taken from [2].

By reversing the polarity of the voltage the two different atom types can be distinguished [1].

2.6 Piezo-effect

For the fine adjustment and the measurement with the tip, very sensible components for the movement are needed. Here they are realised by using Piezo-elements. Piezo-electric crystals have the property that they stretch in one direction and contract in the other direction when exposed to an electric field, because the atoms inside the crystal align. Thereby small and controlled movements are possible by regulated stimulation of the crystal [2].

3 Setup and measurements

To perform the measurements we use a scanning head in which one has to attach a tip under a golden spring. Afterwards the sample is placed on the sample holder and the sample holder is positioned on a motor to move it towards the tip until a preset current is measured. To scan the sample, the tip is moved around the sample with three piezo elements to be able to move in all three dimensions. The used measurement mode is the constant current mode. Due to the setup being really prone to failure because of mechanical and acoustical vibrations, the whole setup is screwed to the wall and the setup stands on a thick damping mat. There is also a box filled with sound insulation, which is put on top of the setup, to minimise the acoustical vibrations. The setup can be seen in Figure 7 and a zoomed in picture of the scanning head can be found in Figure 8.

Fig. 7: On the left hand side the electronics of the setup are shown and on the right hand side one can see the scanning head with a sample inside of it. This graphic is taken from [1].

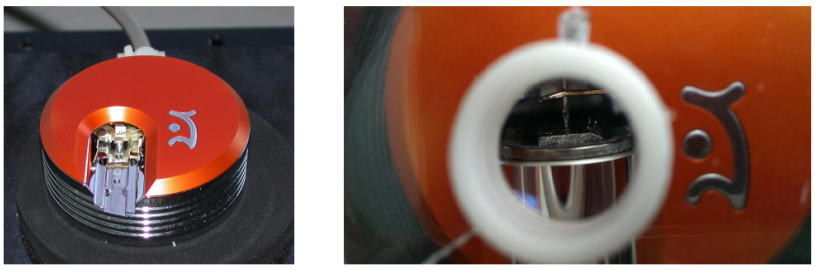

Fig. 8: In the left graphic the scanning head is presented. In the right graphic a close-up picture of the tip on the top and below the sample on the sample holder can be found. This graphic is taken from [1].

The tip is moved on a raster with the piezo elements to scan the sample. The scanning raster of the tip can be found in Figure 9.

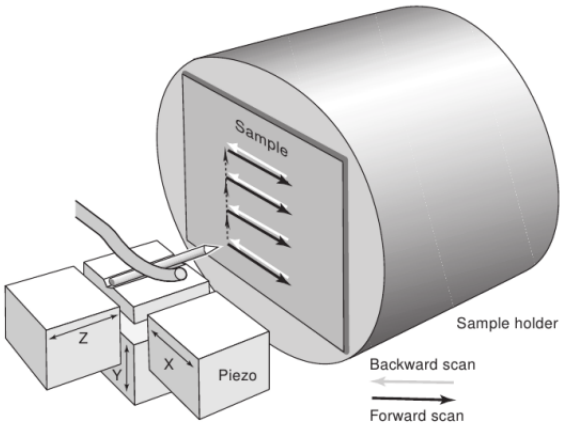

Fig. 9: In this graphic one can see the scanning raster of the clamped tip, which is achieved with the three piezo elements. Every line is measured forwards and backwards. This graphic is taken from [1].

To perform the measurements, the first step is to clean every surface in the scanning head with alcohol. Afterwards one has to produce a tip which should be as close to one atom as possible. After clamping it under the golden spring in the scanning head, the sample is put on the sample holder and then the sample holder is placed on the motor at a distance of around 3 mm to the tip. With the help of a magnifying lens the sample is moved with the `Advance`-mode in the `easyScan 2 STM` software to a distance of roughly 1 mm. Afterwards the `Approach`-mode of the software is used until the preset current of 1 nA is measured. The actual measurement is then performed in the constant current mode and with a tip voltage of 54 mV. The other measurement parameters, such as the image width, the measuring time per line, the points per line and the rotation of the tip, are varied from measurement to measurement and can be found in Table 2 in the appendix.

The measurement with graphite is the first one to be performed and because of the clear structure of graphite one should use this measurement to assess the quality of the tip. Afterwards the gold and the MoS_2 can be measured with a good tip. A difference in the measurement of the MoS_2 is, that one time the applied voltage is reversed to distinguish between the two atoms.

4 Data analysis and discussion of uncertainties

In the two days of the measurement only very noisy and blurry images have been created and no analysable data was measured. Hence the focus on the measurement lays on the graphite sample which should provide the best image and for the other two samples no measurements where taken. Still in the following section, a part about the gold and MoS_2 samples is added to show what results would have been expected and how this data would have been analysed. A detailed discussion of the problems and possible solutions are presented in subsection 5.2.

4.1 Measurement of the graphite sample

4.1.1 Preparations of the measurements

With the graphite sample all in all 44 measurements where performed. Since no usable data could have been taken, the whole process of measuring focused on improvements of the previous measurements. Since the measurement is mostly dependent of the quality of the tip, after hitting the sample with a good tip, the measurements have to start from the beginning with a new tip. For all the measurements the data was prepared with the software `Gwyddion` and a filter that levels all the data by subtraction of the mean was apllied. Afterwards graphics of all the measurements were exported and can be found in the appendix (Figure 16 to Figure 59).

An overview of all the measurements with the tips and parameters used, as well as a short comment on the problems, progress and other aspects can also be found in the appendix in Table 2. After some starting measurements (Figure 16 to Figure 19) on the first day, only two other tips were used (Figure 20 to Figure 35). On the second day several other tips were produced and tested. Except for two promising tips with quite stable pictures (Figure 41 to Figure 45 and Figure 53 to Figure 59), for the other tips only few measurements were taken to get a first impression.

4.1.2 Exemplary analysis of the data

For the analysis part of the graphite we can discuss two interesting measurements. First, we look at a measurement from the first day with the first tip that provided stable pictures. As in all the other measurements an atomic structure could not be detected on first sight, but when measuring on a bigger scale, a vertical line gets visible. Two measurements on higher scale are shown in Figure 10.

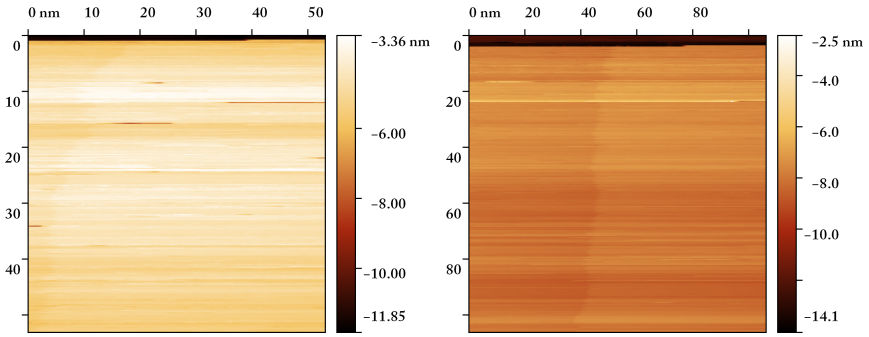

(a) Measurement with a scale of 53 nm

(b) Measurement with a scale of 110 nm

Fig. 10: In this graphics one can see the fifth and sixth measurement with the first tip that provided stable pictures. Both of them are on a bigger scale with the one on the left having a scale of 53 nm and the other one having a scale of 110 nm. On both pictures a vague vertical line can be observed.

By finding this line in two independent measurements one can be sure that it is a surface structure of the graphite. While the tip for this measurement was not sharp enough to get high resolution pictures on atomic scale, bigger structure could have been measured.

The other data analysed in this part comes from a measurement of the second day. It is the measurement with the most stable picture and can be found in Figure 11.

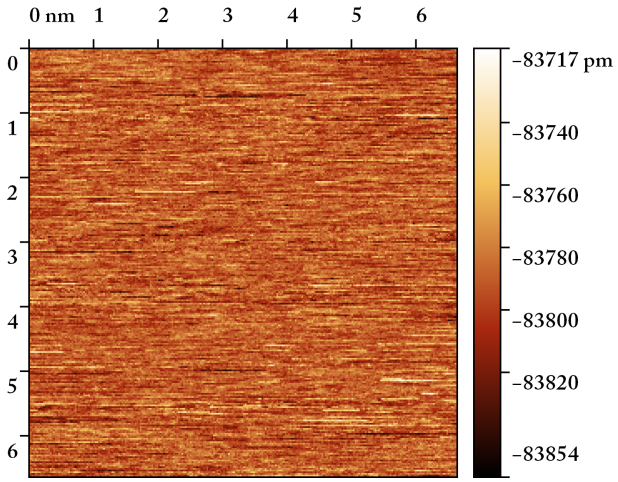

Fig. 11: In this graphic one can see the first measurement with the fifth tip that provided very stable pictures. It is measured on a scale of 6.6 nm with a scanning time of 0.4 s and 256 points per line.

In a good measurement one could take the data and apply a 2D-FFT-Filter in `Gwyddion` to get only the frequencies that show the grid of the atom. There one would expect a hexagon of points in the Fourier spectrum and than could filter the image by using only those six points of the spectrum. For our data we get the following spectrum, presented in Figure 12.

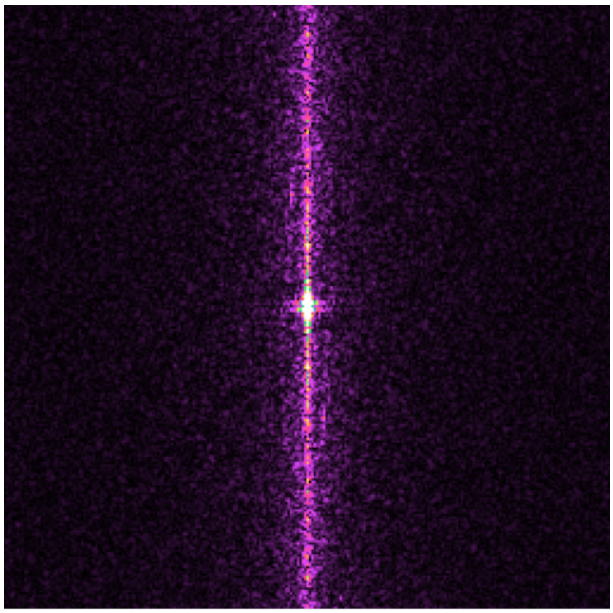

Fig. 12: In this graphic one can see the Fourier transformation of the most stable picture. A lot of noise is recognisable in this image and therefore it is impossible to filter the correct frequencies.

It is nearly impossible to identify any hexagonal structure in the data which means a correction

of the data is not possible by using this filter. This holds true for all the other measurements too. In a next step one would take the distance between two maxima on the surface to find the lattice constant d. Therefore again the software `Gwyddion` can be used. To show this, in Figure 13 some random distances in our measurement are taken with `Gwyddion`.

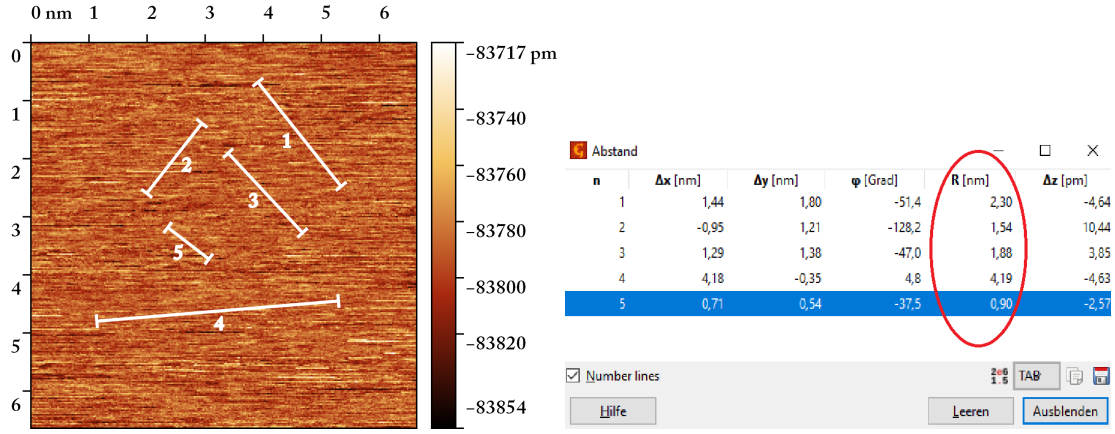

(a) Random measurements in the data (b) Measured lengths l provided by `Gwyddion`

Fig. 13: In the left graphic an exemplary measurements with `Gwyddion` is taken in the data of the most stable picture. In the right graphic the measured lengths l are marked in a red circle.

To find the lattice constant d from this measurement one has to divide the measured length l by the number of minima m between the marked maxima with the following equation:

$$d = \frac{l}{m}. \tag{10}$$

To get an exacter measurement of the lattice constant one should measure multiple lengths between multiple maxima and form a mean [8]:

$$\tilde{d} = \frac{1}{n}\sum_{i}^{n} d_i. \tag{11}$$

The uncertainty can then be found by calculating the standard deviation of the mean [8]:

$$\Delta\tilde{d} = \frac{1}{\sqrt{n}}\sqrt{\frac{\sum_i^n (d_i - \tilde{d})^2}{n-1}}. \tag{12}$$

4.2 Measurement of the gold sample

The measurement of the gold sample couldn't be performed due to not having a sharp enough tip for measurements, so an example for a measurement of gold is taken from [2] and can be seen in Figure 14.

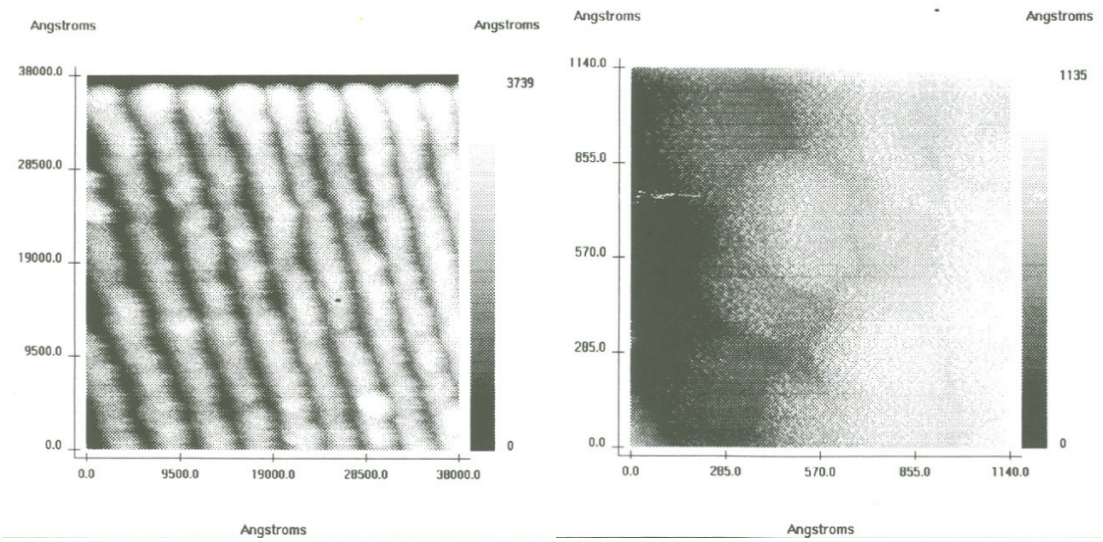

(a) Surface of gold on a 38 000 Å scale from [2] (b) Surface of gold on a 1140 Å scale from [2]

Fig. 14: In this graphics one can see the expected measurements of the gold surface structure taken from [2]. In the left image lines of gold are presented with a gap of approximately 4000 Å. In the right image a cloudy structure is observed.

The surface of the sample is coated with lines of gold and therefore has a linear structure when measuring a bigger area as seen in Figure 14a. The atomic structure of the gold isn't expected to be measured, because when a voltage is applied to a metal the electrons are delocalized and have very small fluctuations in their density in the sample. These fluctuations have an order of approximately 0.1 Å [2] and thus can't be measured with the used setup. This can already be seen in Figure 14b in which only cloudy patterns are recognisable.

4.3 Measurement of the MoS_2 sample

This measurement also hasn't been taken due to no good enough tip. In this part one can take two different measurements. The first measurement is conducted with a normal voltage and the second one with an inverted voltage. Because of the special structure of MoS_2 the tunnelling either takes place between the sulphur and the tip or the molybdenum and the tip. Therefore one can measure the structure of the sulphur layer or the structure of the molybdenum layer by applying differently polarised voltages. An example picture with only one voltage set for the measurement is presented in Figure 15, again taken from [2].

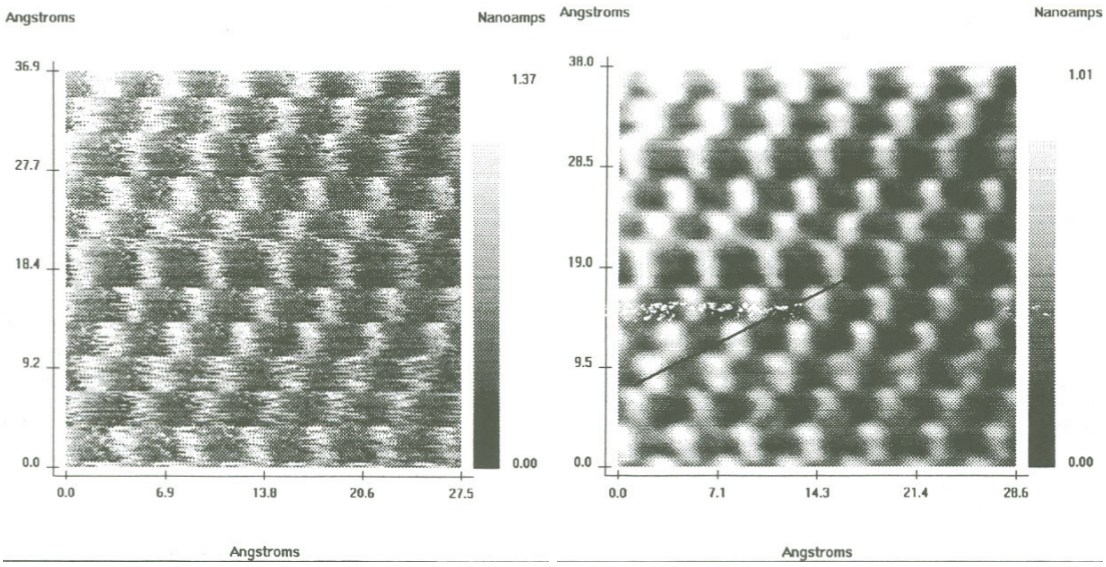

(a) Unfiltered picture of the MoS_2 surface from [2]

(b) Filtered picture of the MoS_2 surface from [2]

Fig. 15: In the two pictures the surface of MoS_2 on approximately 37 $Å^2$ is portrayed to give an impression of the MoS_2-measurement. It is measured with only one voltage set. On the left hand side the raw data is presented, whereas on the right side a filter is applied. The graphic is taken from [2].

The analysis of these structures can be performed analogously to the graphite with the filtering in the Fourier transformation and the formulas for the lattice constant (Equation 10), the mean of the lattice constant (Equation 11) and it's uncertainty (Equation 12).

5 Summary and discussion of the results

5.1 Summary of the results

For the measuring of the graphite probe only little data that shows anything relevant was taken. Therefore a real analysis of the data and the determination of a grating constant were not successful. Still in the main part, a description is given, how that data would have been analysed. The main part of the measuring time was used to optimise the measurements by creating new tips and changing parameters to get the best out of any tip. Still no good tip could have been created, thus for the two other samples not a single measurement was proceeded.

5.2 Discussion of results and uncertainties

As already seen in the previous chapters, the measurement could not be performed properly and no meaningful data has been taken so no scientific results can be presented. For the graphite sample multiple measurements with different parameters and different tips only lead to very noisy data that could only be evaluated superficially. The other samples could not be measured at all in lack of a good setup that was not found during the graphite measurements. Therefore in the following section different aspects that lead to problems while measuring and possible solutions will be discussed.

The first and also greatest problem with the measuring is the production of the tip. In the experiment guidance made available by the lab team it says: *„Die wesentliche Herausforderung bei der Tunnelmikroskopie ist die Präparation der Platin-Iridium-Spitze. Sie ist mehr oder weniger dem Zufall überlassen. “* ([1], p. 1, translation: *„The main challenge in tunnelling microscopy is the preparation of the platinum-iridium tip. It's more or less left to chance.“*). This statement holds true perfectly: While it is of course possible to influence the quality of the tip by using several different strategies and tools, still only a small fraction of the produced tips could provide any picture on the screen. In addition, also tips that on first sight looked very promising could not always produce better pictures. A possibility to improve the measurement would be the usage of a better magnifying glass or even a light microscope to control the quality of the tip. Of course better results could also be achieved by using tips not produced by hand, because on the one hand the quality of the pictures would increase dramatically and on the other hand one could focus on all the other parameters that could be improved. The disadvantage of course would be the high costs of industrially produced tips.

The second main source of error is the approach of the tip to the sample. While approaching the sample by hand is not really a problem, the approach with the `Advance/Retract` buttons is very difficult to perform, because the stopping point is very hard to estimate. If the tip is too far away from the sample, the approaching time can get really high (up to an hour) and if it is too near, the danger of hitting the sample with the tip gets higher.

Also the third approaching step with the `Approach` button often lead to unusable measurements because either the tip hit the sample and the indicator light gets red or the approach stopped at some point and the light gets orange. In the case of an orange light it is hard to find out what the real problem is and one has to try another approach, maybe after cleaning the setup or rotating the sample. Also finding the right approaching speed turned out to be very difficult. Too high approaching speech often lead to the tip driving directly into the sample, whereas too low approaching speed could lead to very high approaching times. It would have been helpful to know the absolute speed of the approach to get a better estimation for the time it takes.

The last important point that has to be discussed is the choice of the parameters used for the measurement. For the quality and the measuring time per line it is always a weighing up between quality and measuring time. Whereas on the first day we tried to get good pictures by taking high resolutions and measuring times, for the second day we focused more on finding a good

tip to perform measurements. Therefore with some of the tips we only took one or two low quality measurements to get a first impression. It could have been more rational to also focus on different parameters and not only on the first impression of the pictures, but on the other hand the measurement depends deeply on the quality of the tip and it is not really sensible to focus too much on low quality tips.

Other parameters that could have been used more in the measurement are the rotation, the voltage and the current. For the voltage and the current, a change in these values often only caused a higher amplitude of the measurement which is not very useful if the whole measurement is very noisy. The rotation on the other hand could produce very different pictures and it would have been sensible to focus more on the rotation, especially since the tips do not have the shape of a cone but more of a cut cylinder. The problem with this parameter is, that it is also more or less random, so focusing on this parameter also costs a lot of time.

Other parameters that maybe could have improved the measurement but are not as relevant as the ones before are acoustic aspects such as noise we produced or noise from outside the building, thermal variations over the day, dirt in the air or in the setup and mechanical vibrations that can be caused for example by people walking through the building.

All in all the main difficulty in the performance of the experiment is the consideration between performing detailed and high quality measurements and the time it takes to do the measurements. In almost all the aspects of the experiment (producing the tip, approaching the tip, measuring with the software) performing a good measurement takes a lot of time. On the other hand, because the true quality of the tip can only be found after measuring, a lot of time is needed to find a tip good enough for the measurements. Time management and endurance are thereby the most important aspect of the experiment.

References

[1] M. Köhli, S. Röttinger: *Rastertunnelmikroskop – Versuchsanleitung Fortgeschrittenen Praktikum Teil 1*, (Freiburg im Breisgau: 2013)

[2] D. Ritzmann: *Einrichtung eines Versuchs: Rastertunnelmikroskopie für das Fortgeschrittenen-Praktikum 2*, (Freiburg im Breisgau: 1994)

[3] Prof. Dr. G. Stock: *Skript zur Vorlesung – Theoretische Physik III: Quantenmechanik*, (Freiburg im Breisgau: 2022)

[4] W.Demtröder: *Experimentalphysik 3 - Atome, Moleküle und Festkörper*, 5th edition, (Berlin, Heidelberg: Springer Spektrum, 2016)

[5] T. Güner: *Entropic Tunneling Time and its Applications* https://www.researchgate.net/publication/308784586_Entropic_Tunneling_Time_and_its_Applications (Izmir: 2014, accessed on 5.9.2022)

[6] F. Trixler: *Quantum Tunnelling to the Origin and Evolution of Life* https://www.researchgate.net/publication/256613933_Quantum_Tunnelling_to_the_Origin_and_Evolution_of_Life (Munich: 2013, accessed on 5.9.2022)

[7] V. Mironov: *Fundamentals of Scanning Probe Microscopy* https://www.researchgate.net/publication/317042630_Fundamentals_of_Scanning_Probe_Microscopy (Nizhniy Novgorod: 2004, accessed on 5.9.2022)

[8] Dr. Christof Bartels, Dr. Lukas Bruder, Dr. Thomas Pfohl: *Datenanalyse Teil A - Skript zur Vorlesung am 06.09.2021*, (Freiburg im Breisgau: 2021/22)

[9] Dr. Christof Bartels, Dr. Lukas Bruder, Dr. Thomas Pfohl: *Datenanalyse Teil B - Skript zur Vorlesung am 28.02.2022*, (Freiburg im Breisgau: 2021/22)

7 Attachment

7.1 Table of all adjusted parameters for the measurements

Tab. 2: Table of the adjusted parameters for the measurements. In this table the number of the measurement, the figure, the tip, the measuring scale, the time per line, the resolution, the tip rotation and comments are listed for each measurement.

No.	Figure	Tip	Scale	Time	Resolution	Rotation	Comments
1	Figure 16	-	6.6 nm	0.2 s	128	0°	not close enough to sample
2	Figure 17	-	6.6 nm	0.2 s	128	0°	first image, very noisy
3	Figure 18	-	6.6 nm	0.2 s	128	0°	tip crashed sample
4	Figure 19	-	6.6 nm	0.2 s	128	0°	too much noise
5	Figure 20	1	6.6 nm	0.2 s	128	0°	noisy picture: new parameters
6	Figure 21	1	6.6 nm	0.4 s	256	0°	higher resolution
7	Figure 22	1	6.6 nm	0.4 s	512	0°	higher resolution
8	Figure 23	1	6.6 nm	0.8 s	128	0°	higher time constant
9	Figure 24	1	53 nm	0.4 s	256	0°	bigger scale
10	Figure 25	1	0.11 µm	0.4 s	256	0°	bigger scale
11	Figure 26	1	6.6 nm	0.4 s	256	45°	rotation, no analysable data, new tip
12	Figure 27	2	6.6 nm	0.4 s	256	0°	-
13	Figure 28	2	53 nm	0.4 s	256	0°	bigger scale
14	Figure 29	2	3.3 nm	0.4 s	512	0°	higher resolution, smaller scale
15	Figure 30	2	3.3 nm	0.2 s	256	20°	trying different rotations
16	Figure 31	2	3.3 nm	0.2 s	256	−20°	-
17	Figure 32	2	3.3 nm	0.2 s	256	10°	-
18	Figure 33	2	3.3 nm	0.2 s	256	5°	-
19	Figure 34	2	3.3 nm	0.2 s	256	85°	-
20	Figure 35	2	13 nm	0.2 s	256	85°	bigger scale
21	Figure 36	3	6.6 nm	0.4 s	256	0°	day 2, new tip
22	Figure 37	3	6.6 nm	0.4 s	256	20°	rotation
23	Figure 38	4	6.6 nm	0.4 s	256	0°	-
24	Figure 39	4	6.6 nm	0.4 s	256	−50°	rotation
25	Figure 40	4	27 nm	0.4 s	256	0°	bigger scale
26	Figure 41	5	6.6 nm	0.4 s	256	0°	promising tip, stable picture
27	Figure 42	5	13 nm	0.4 s	256	0°	bigger scale
28	Figure 43	5	13 nm	0.4 s	256	−20°	rotation
29	Figure 44	5	53 nm	0.4 s	256	0°	bigger scale
30	Figure 45	5	3.3 nm	0.4 s	256	0°	smaller scale variation of rotation, voltage, current ⇒ no change in sharpness
31	Figure 46	6	6.6 nm	0.4 s	256	0°	very unstable picture
32	Figure 47	7	6.6 nm	0.4 s	256	0°	very unstable picture
33	Figure 48	9	6.6 nm	0.4 s	256	0°	approaching problem
34	Figure 49	9	6.6 nm	0.4 s	256	−20°	new approaching
35	Figure 50	10	6.6 nm	0.4 s	256	0°	noisy street sweeper
36	Figure 51	10	6.6 nm	0.4 s	256	0°	⇒ visible in pictures
37	Figure 52	11	6.6 nm	0.4 s	256	0°	not analysable
38	Figure 53	12	6.6 nm	0.4 s	256	0°	-
39	Figure 54	12	6.6 nm	0.8 s	128	−50°	variation of time, resolution, rotation
40	Figure 55	12	6.6 nm	0.2 s	512	−50°	variation of time, resolution
41	Figure 56	12	6.6 nm	0.4 s	256	50°	variation of time, resolution, rotation
42	Figure 57	12	6.6 nm	0.3 s	256	33°	variation of time, rotation
43	Figure 58	12	6.6 nm	0.3 s	256	90°	variation of rotation
44	Figure 59	12	6.6 nm	0.3 s	256	110°	variation of rotation

7.2 First unsuccessful measurements

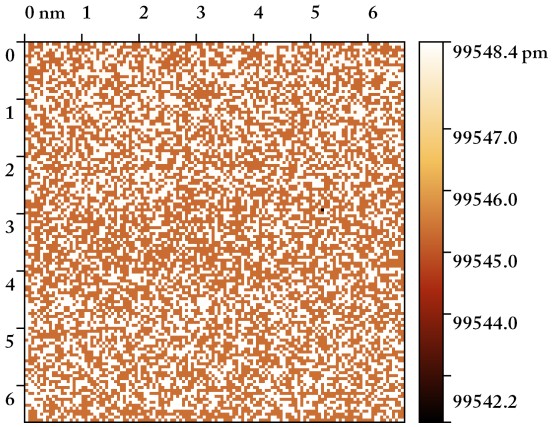

Fig. 16: First unsuccessful measurement without getting a real signal.

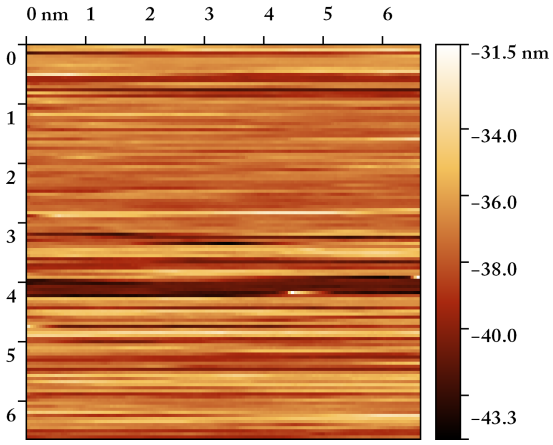

Fig. 17: Second unsuccessful measurement with a lot of noise and no clear signal.

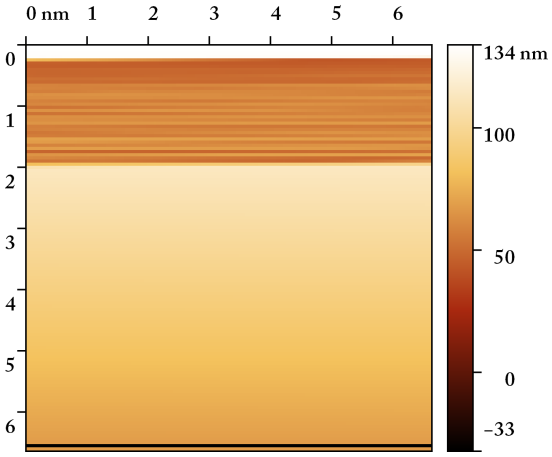

Fig. 18: Third unsuccessful measurement with the tip driving into the sample while measuring.

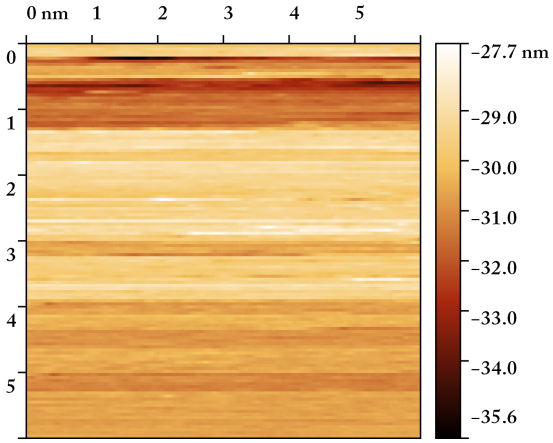

Fig. 19: Fourth unsuccessful measurement with a lot of noise and no clear signal.

7.3 Measurements with the first tip

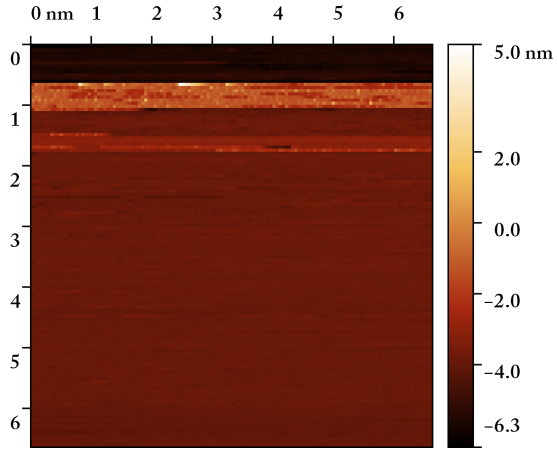

Fig. 20: Measurement 1 on graphite with the first tip. The scale is at 6.6 nm, the time constant at 0.2 s and 128 points per line are taken. The data is already stabilised and corrected as described in the main part.

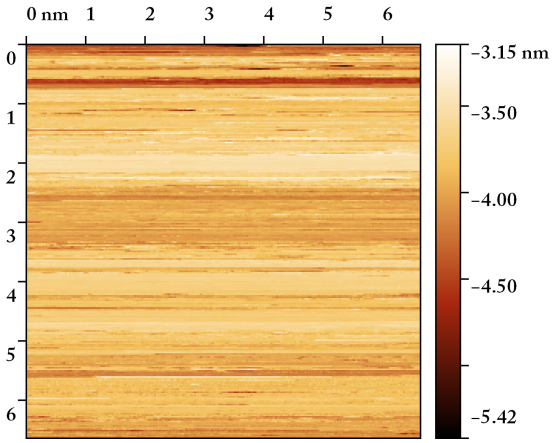

Fig. 21: Measurement 2 on graphite with the first tip. The scale is at 6.6 nm, the time constant at 0.4 s and 256 points per line are taken. The data is already stabilised and corrected as described in the main part.

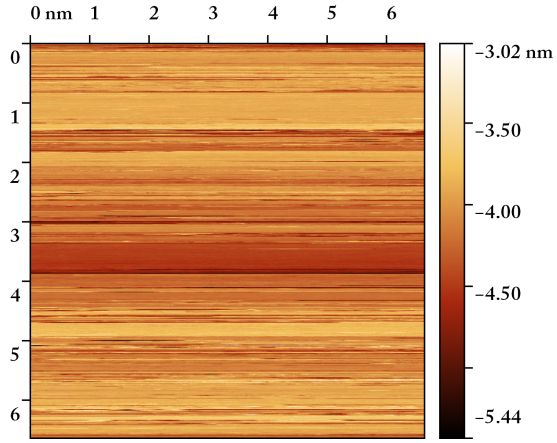

Fig. 22: Measurement 3 on graphite with the first tip. The scale is at 6.6 nm, the time constant at 0.4 s and 512 points per line are taken. The data is already stabilised and corrected as described in the main part.

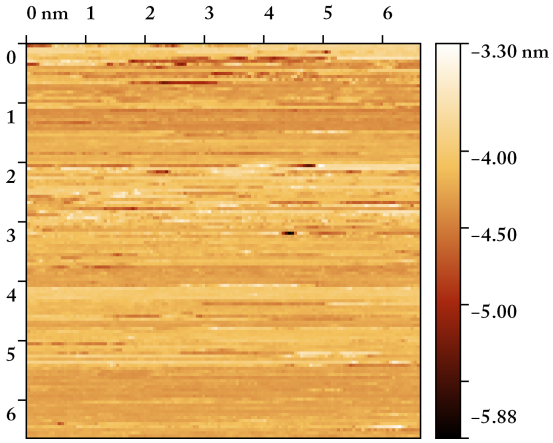

Fig. 23: Measurement 4 on graphite with the first tip. The scale is at 6.6 nm, the time constant at 0.8 s and 128 points per line are taken. The data is already stabilised and corrected as described in the main part.

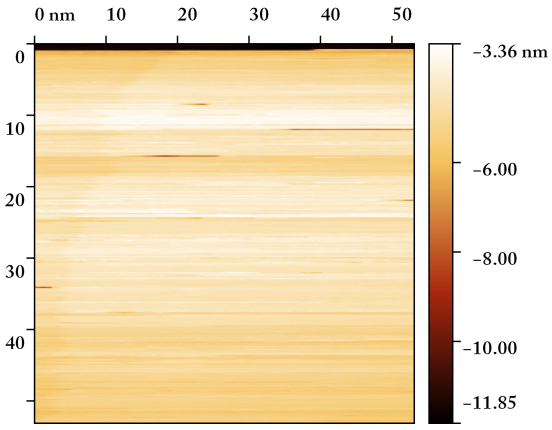

Fig. 24: Measurement 5 on graphite with the first tip. The scale is at 53 nm, the time constant at 0.4 s and 256 points per line are taken. The data is already stabilised and corrected as described in the main part.

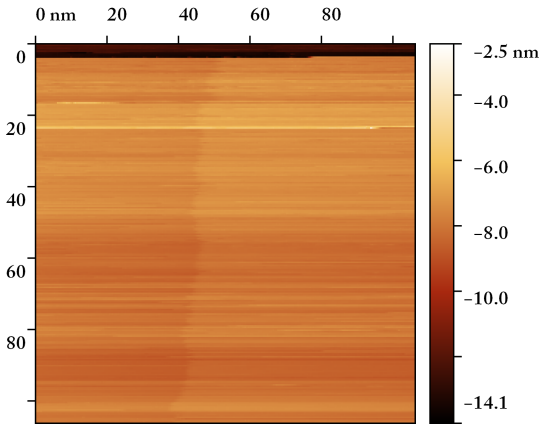

Fig. 25: Measurement 6 on graphite with the first tip. The scale is at 0.11 µm, the time constant at 0.4 s and 256 points per line are taken. The data is already stabilised and corrected as described in the main part.

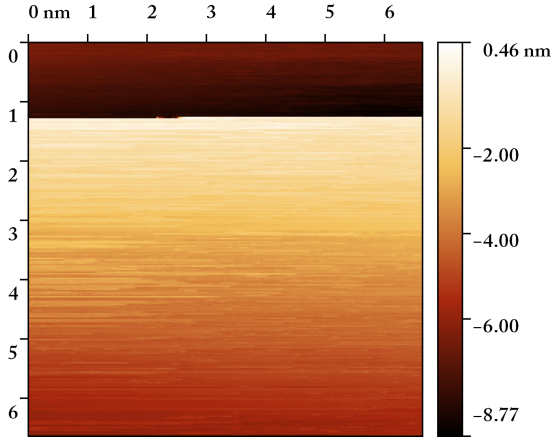

Fig. 26: Measurement 7 on graphite with the first tip. The scale is at 6.6 nm, the time constant at 0.4 s and 256 points per line are taken with a tip rotation of 45°. The data is already stabilised and corrected as described in the main part.

7.4 Measurements with the second tip

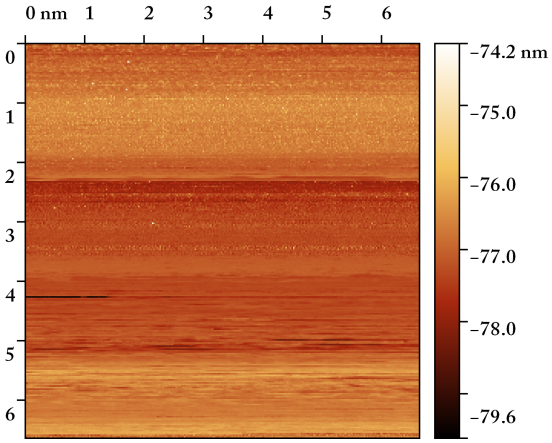

Fig. 27: Measurement 1 on graphite with the second tip. The scale is at 6.6 nm, the time constant at 0.4 s and 256 points per line are taken. The data is already stabilised and corrected as described in the main part.

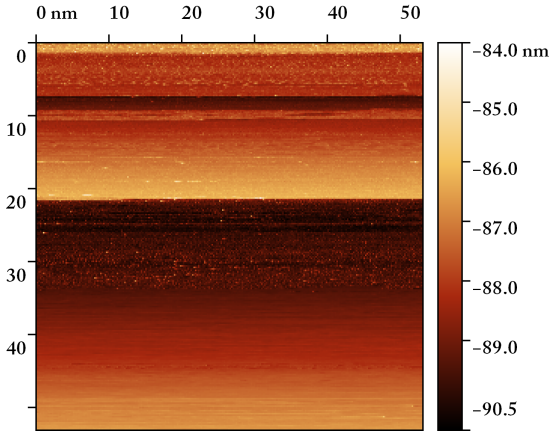

Fig. 28: Measurement 2 on graphite with the second tip. The scale is at 53 nm, the time constant at 0.4 s and 256 points per line are taken. The data is already stabilised and corrected as described in the main part.

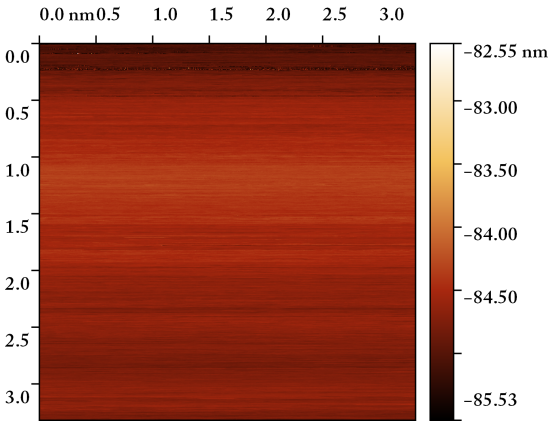

Fig. 29: Measurement 3 on graphite with the second tip. The scale is at 3.3 nm, the time constant at 0.4 s and 512 points per line are taken. The data is already stabilised and corrected as described in the main part.

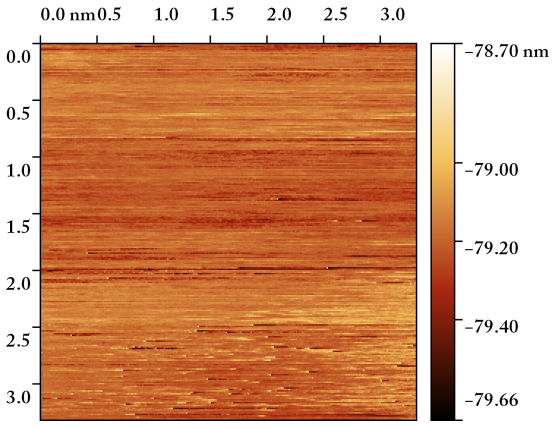

Fig. 30: Measurement 4 on graphite with the second tip. The scale is at 3.3 nm, the time constant at 0.2 s and 256 points per line are taken with a tip rotation of 20°. The data is already stabilised and corrected as described in the main part.

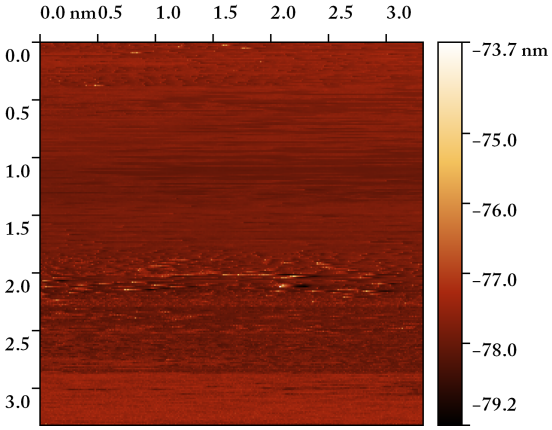

Fig. 31: Measurement 5 on graphite with the second tip. The scale is at 3.3 nm, the time constant at 0.2 s and 256 points per line are taken with a tip rotation of −20°. The data is already stabilised and corrected as described in the main part.

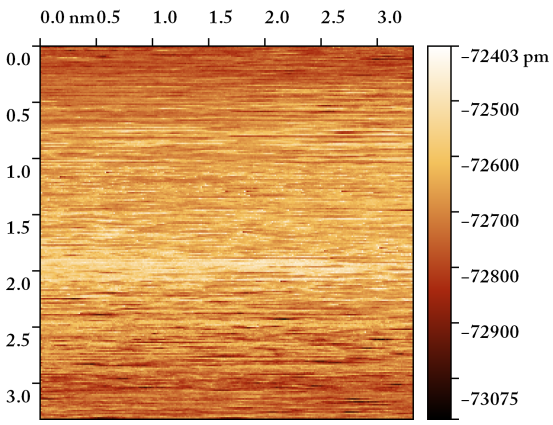

Fig. 32: Measurement 6 on graphite with the second tip. The scale is at 3.3 nm, the time constant at 0.2 s and 256 points per line are taken with a tip rotation of 10°. The data is already stabilised and corrected as described in the main part.

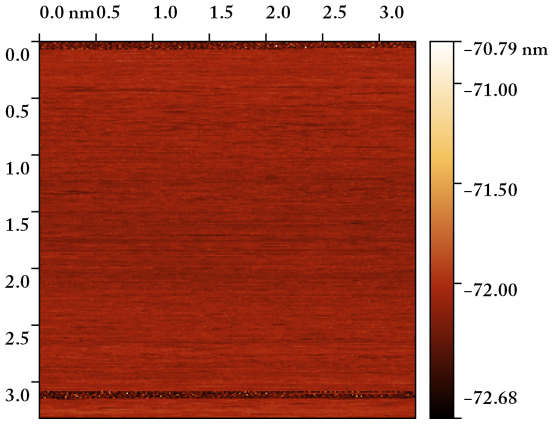

Fig. 33: Measurement 7 on graphite with the second tip. The scale is at 3.3 nm, the time constant at 0.2 s and 256 points per line are taken with a tip rotation of 5°. The data is already stabilised and corrected as described in the main part.

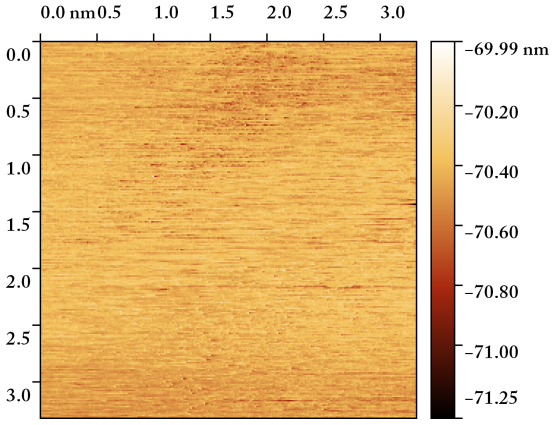

Fig. 34: Measurement 8 on graphite with the second tip. The scale is at 3.3 nm, the time constant at 0.2 s and 256 points per line are taken with a tip rotation of 85°. The data is already stabilised and corrected as described in the main part.

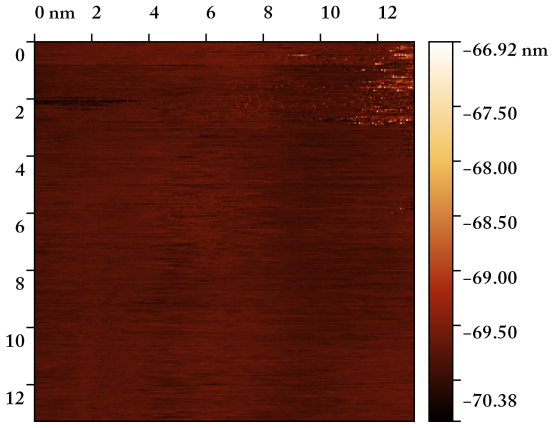

Fig. 35: Measurement 9 on graphite with the second tip. The scale is at 13 nm, the time constant at 0.2 s and 256 points per line are taken with a tip rotation of 85°. The data is already stabilised and corrected as described in the main part.

7.5 Measurements with the third tip

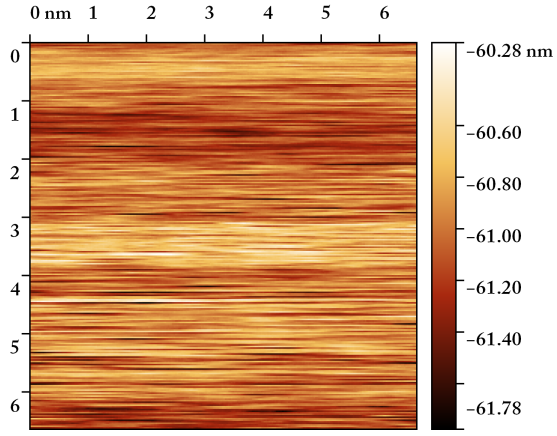

Fig. 36: Measurement 1 on graphite with the third tip. The scale is at 6.6 nm, the time constant at 0.4 s and 256 points per line are taken. The data is already stabilised and corrected as described in the main part.

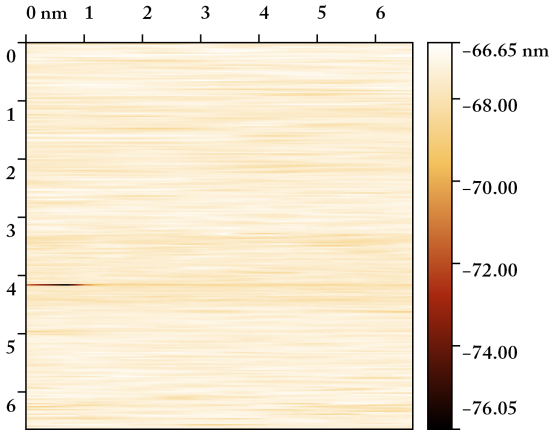

Fig. 37: Measurement 2 on graphite with the third tip. The scale is at 6.6 nm, the time constant at 0.4 s and 256 points per line are taken with a tip rotation of 20°. The data is already stabilised and corrected as described in the main part.

7.6 Measurements with the fourth tip

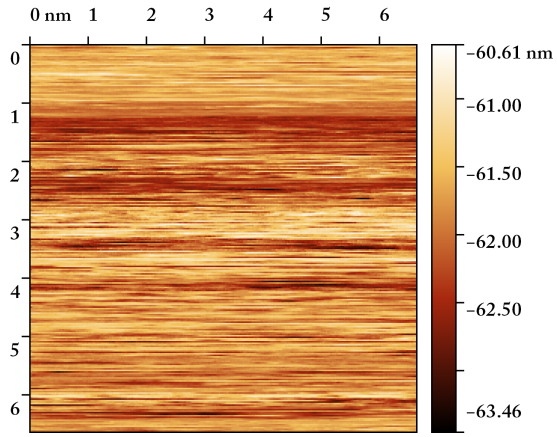

Fig. 38: Measurement 1 on graphite with the fourth tip. The scale is at 6.6 nm, the time constant at 0.4 s and 256 points per line are taken. The data is already stabilised and corrected as described in the main part.

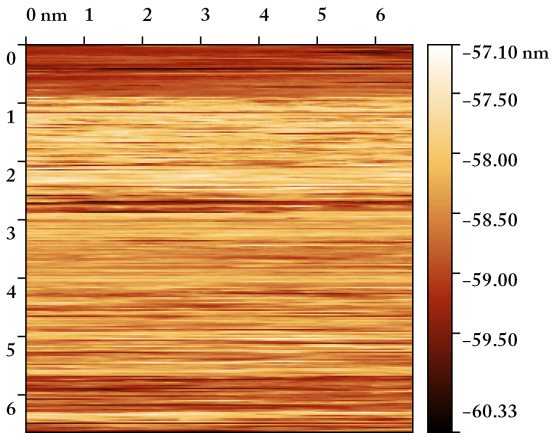

Fig. 39: Measurement 2 on graphite with the fourth tip. The scale is at 6.6 nm, the time constant at 0.4 s and 256 points per line are taken with a tip rotation of 50°. The data is already stabilised and corrected as described in the main part.

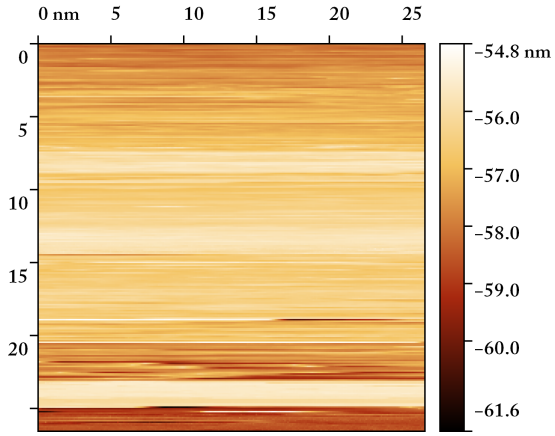

Fig. 40: Measurement 3 on graphite with the third tip. The scale is at 27 nm, the time constant at 0.4 s and 256 points per line are taken. The data is already stabilised and corrected as described in the main part.

7.7 Measurements with the fifth tip

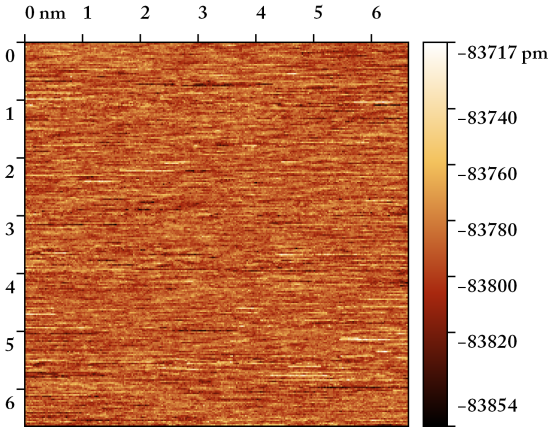

Fig. 41: Measurement 1 on graphite with the fifth tip. The scale is at 6.6 nm, the time constant at 0.4 s and 256 points per line are taken. The data is already stabilised and corrected as described in the main part.

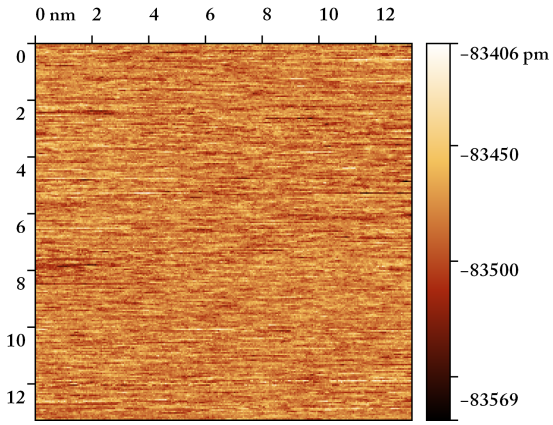

Fig. 42: Measurement 2 on graphite with the fifth tip. The scale is at 13 nm, the time constant at 0.4 s and 256 points per line are taken. The data is already stabilised and corrected as described in the main part.

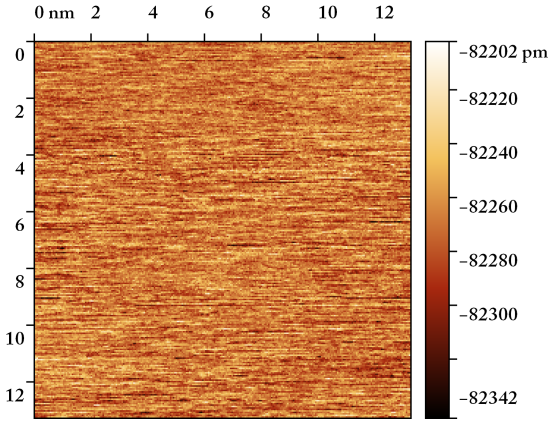

Fig. 43: Measurement 3 on graphite with the fifth tip. The scale is at 13 nm, the time constant at 0.4 s and 256 points per line are taken with a tip rotation of −20°. The data is already stabilised and corrected as described in the main part.

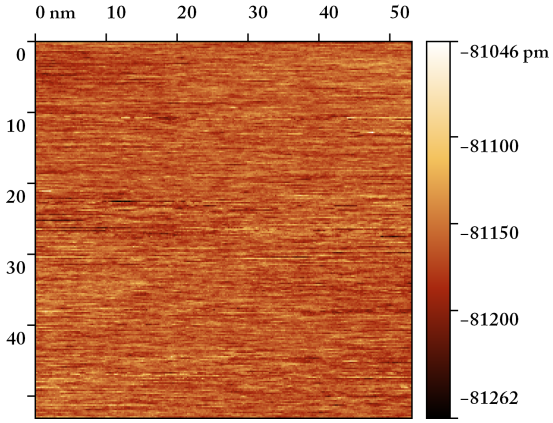

Fig. 44: Measurement 4 on graphite with the fifth tip. The scale is at 53 nm, the time constant at 0.4 s and 256 points per line are taken. The data is already stabilised and corrected as described in the main part.

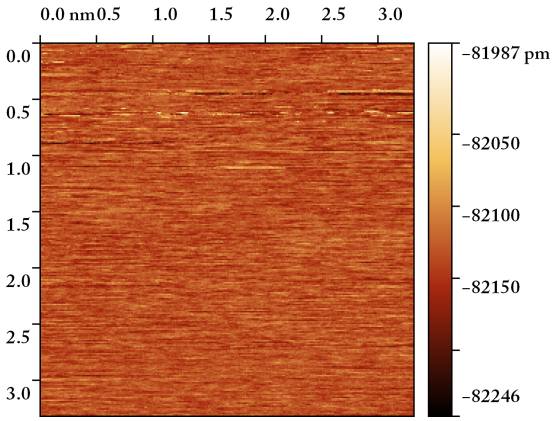

Fig. 45: Measurement 5 on graphite with the fifth tip. The scale is at 3.3 nm, the time constant at 0.4 s and 256 points per line are taken. The data is already stabilised and corrected as described in the main part.

7.8 Measurements with tip 6,7 and 9

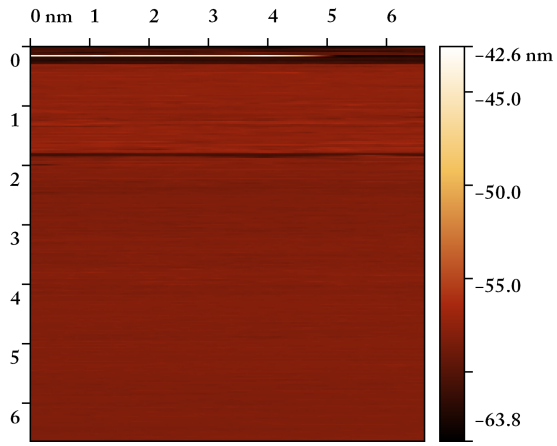

Fig. 46: Measurement on graphite with the sixth tip. The scale is at 6.6 nm, the time constant at 0.4 s and 256 points per line are taken. The data is already stabilised and corrected as described in the main part.

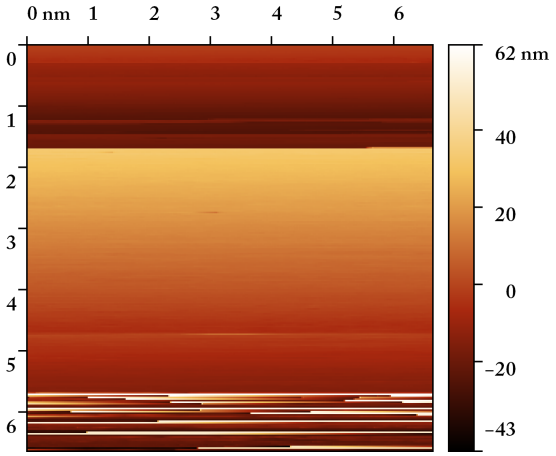

Fig. 47: Measurement on graphite with the seventh tip. The scale is at 6.6 nm, the time constant at 0.4 s and 256 points per line are taken. The data is already stabilised and corrected as described in the main part.

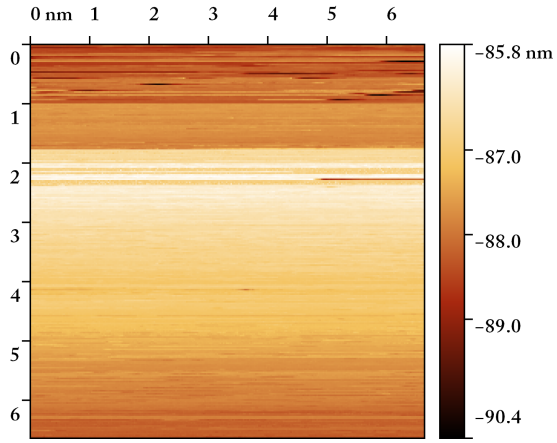

Fig. 48: Measurement 1 on graphite with the ninth tip. The scale is at 6.6 nm, the time constant at 0.4 s and 256 points per line are taken. The data is already stabilised and corrected as described in the main part.

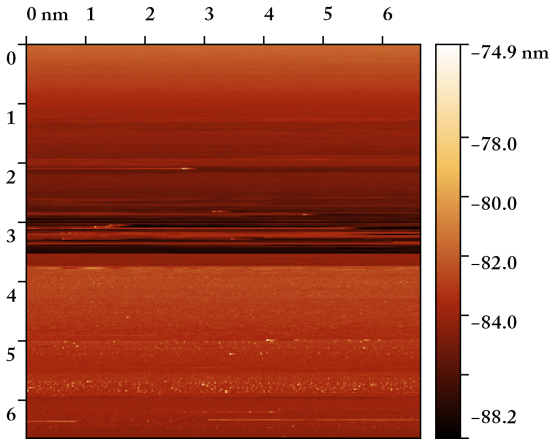

Fig. 49: Measurement 2 on graphite with the ninth tip. The scale is at 6.6 nm, the time constant at 0.4 s and 256 points per line are taken with a tip rotation of $-20°$. The data is already stabilised and corrected as described in the main part.

7.9 Measurements with tip 10 and 11

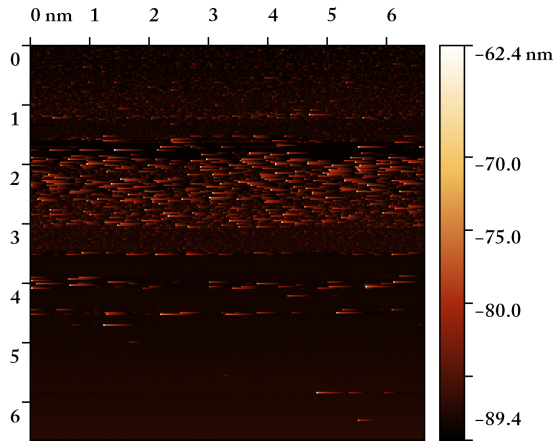

Fig. 50: Measurement 1 on graphite with the tenth tip. The scale is at 6.6 nm, the time constant at 0.4 s and 256 points per line are taken, but with a noisy environment. The data is already stabilised and corrected as described in the main part.

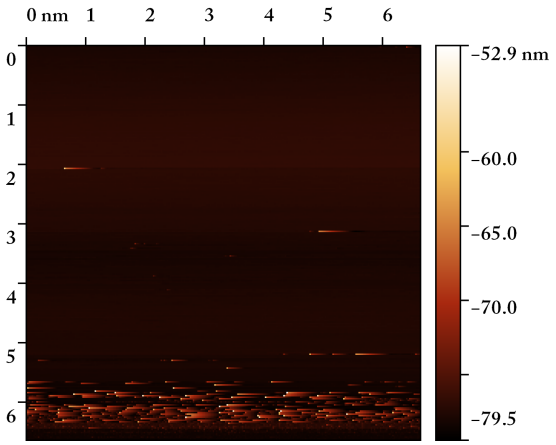

Fig. 51: Measurement 2 on graphite with the tenth tip. The scale is at 6.6 nm, the time constant at 0.4 s and 256 points per line are taken with no noise from the outside. The data is already stabilised and corrected as described in the main part.

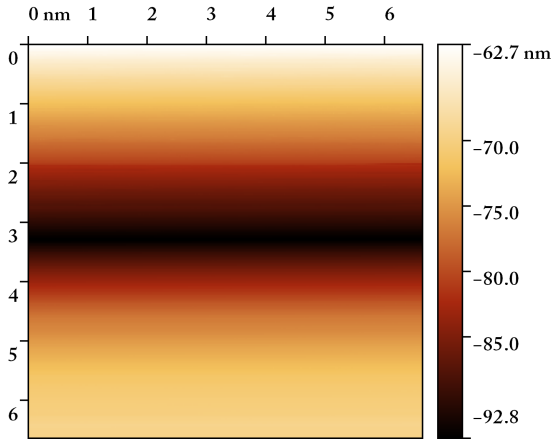

Fig. 52: Measurement on graphite with the eleventh tip. The scale is at 6.6 nm, the time constant at 0.4 s and 256 points per line are taken. The data is already stabilised and corrected as described in the main part.

7.10 Measurements with the twelfth tip

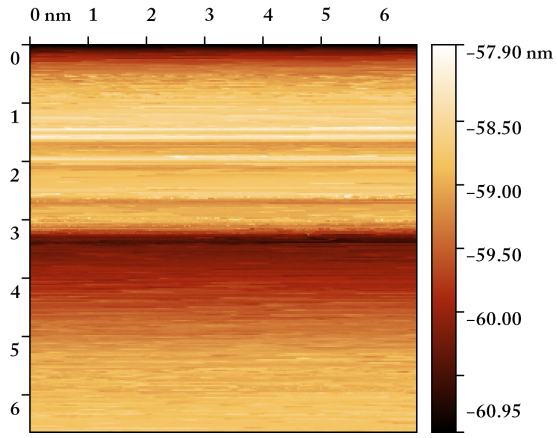

Fig. 53: Measurement 1 on graphite with the twelfth tip. The scale is at 6.6 nm, the time constant at 0.4 s and 256 points per line are taken. The data is already stabilised and corrected as described in the main part.

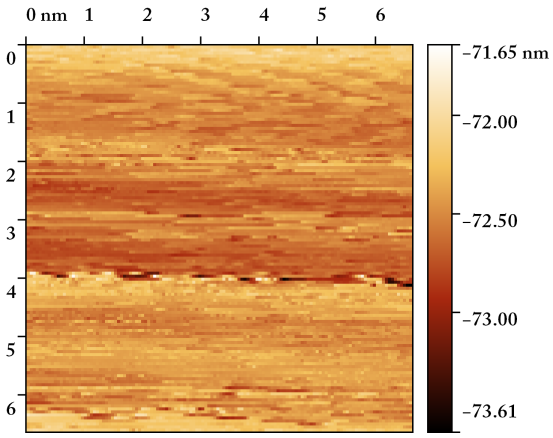

Fig. 54: Measurement 2 on graphite with the twelfth tip. The scale is at 6.6 nm, the time constant at 0.8 s and 128 points per line are taken with a tip rotation of −50°. The data is already stabilised and corrected as described in the main part.

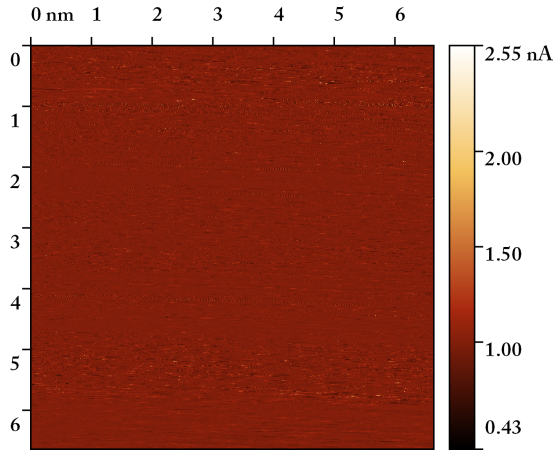

Fig. 55: Measurement 3 on graphite with the twelfth tip. The scale is at 6.6 nm, the time constant at 0.2 s and 512 points per line are taken with a tip rotation of −50°. The data is already stabilised and corrected as described in the main part.

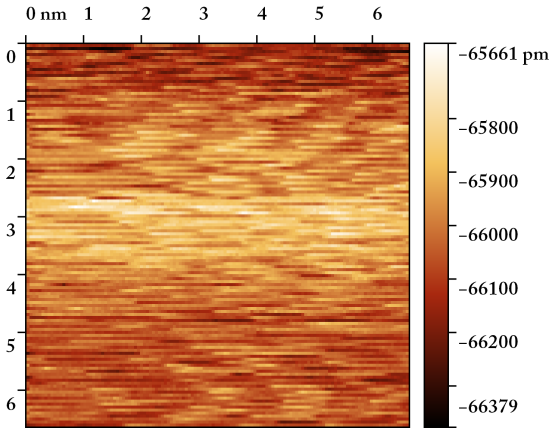

Fig. 56: Measurement 4 on graphite with the twelfth tip. The scale is at 6.6 nm, the time constant at 0.4 s and 256 points per line are taken with a tip rotation of 50°. The data is already stabilised and corrected as described in the main part.

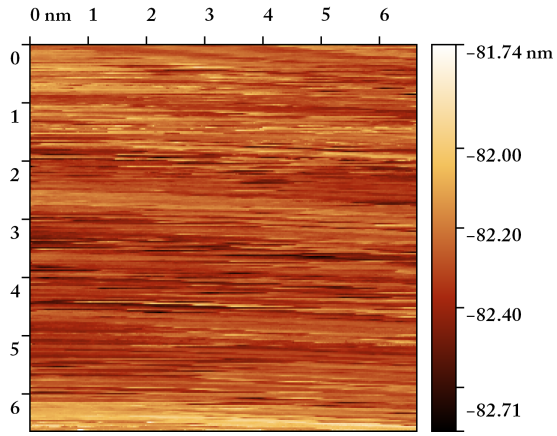

Fig. 57: Measurement 5 on graphite with the first tip. The scale is at 6.6 nm, the time constant at 0.3 s and 256 points per line are taken with a tip rotation of 33°. The data is already stabilised and corrected as described in the main part.

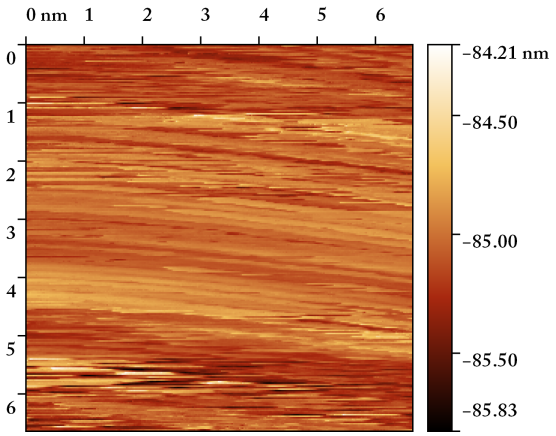

Fig. 58: Measurement 6 on graphite with the twelfth tip. The scale is at 6.6 nm, the time constant at 0.3 s and 256 points per line are taken with a tip rotation of 90°. The data is already stabilised and corrected as described in the main part.

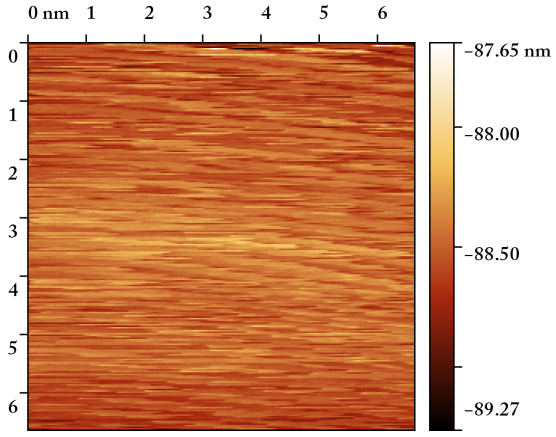

Fig. 59: Measurement 7 on graphite with the twelfth tip. The scale is at 6.6 nm, the time constant at 0.3 s and 256 points per line are taken with a tip rotation of 110°. The data is already stabilised and corrected as described in the main part.

7.11 Lab notes

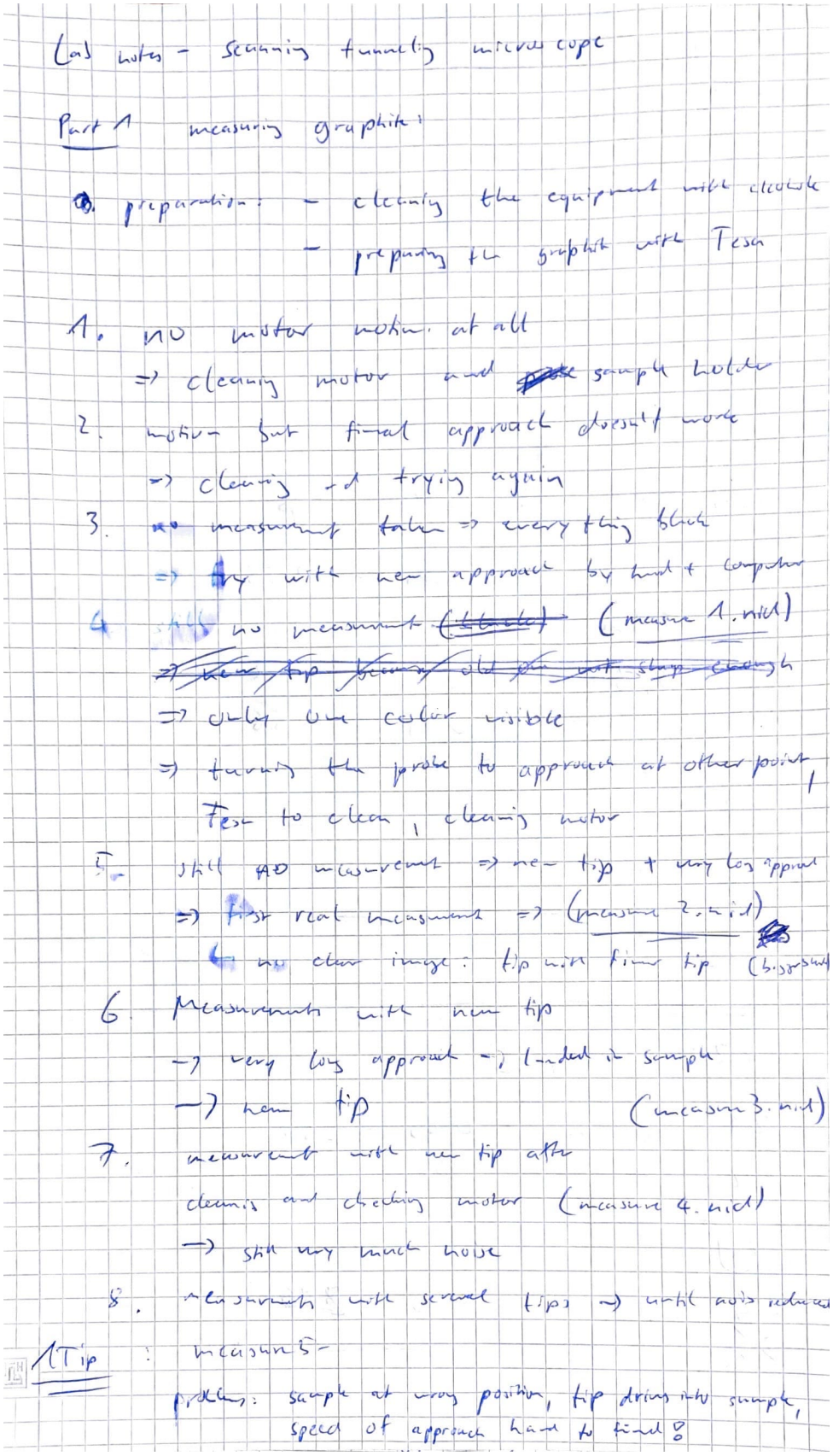

Fig. 60: Lab notes - page 1

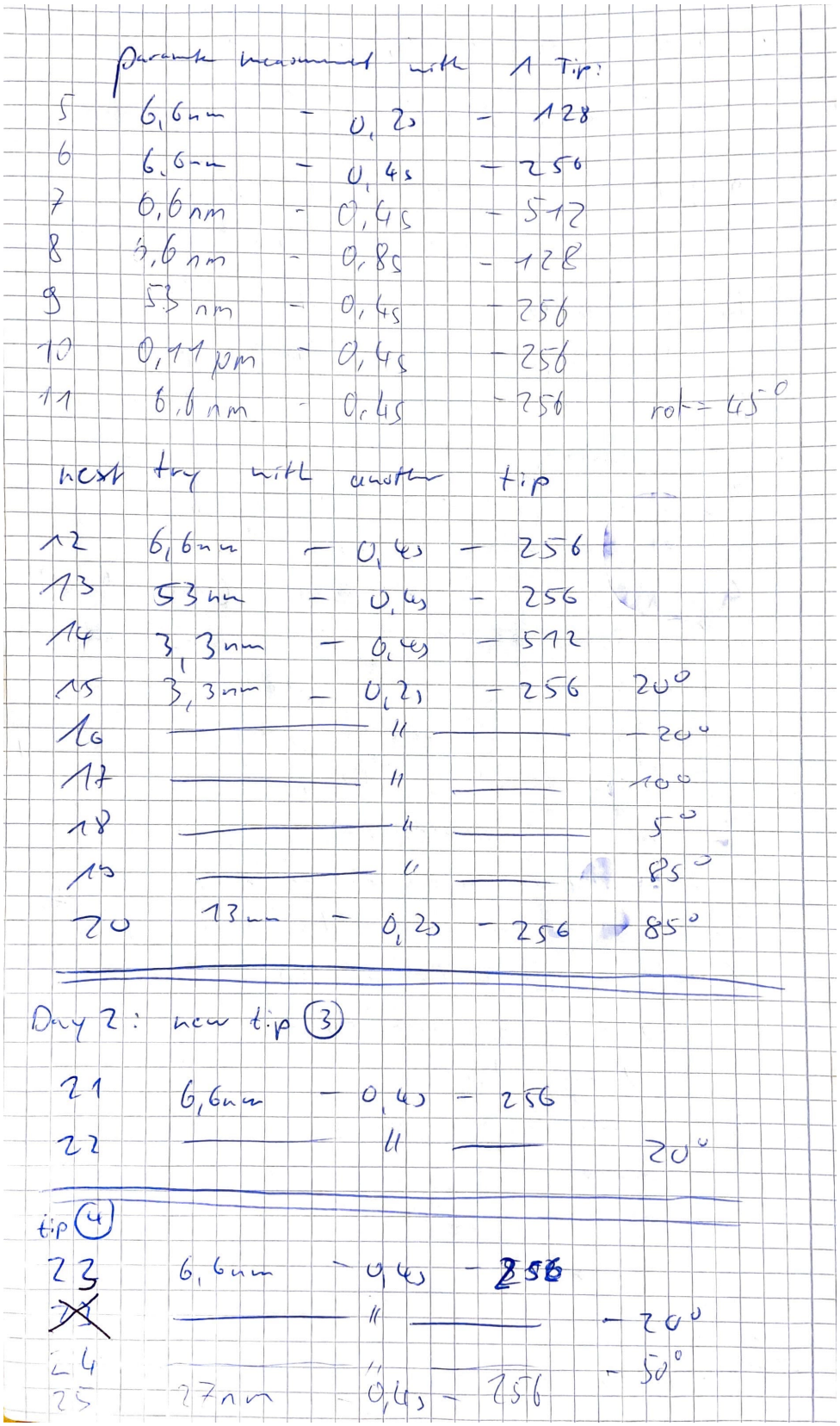

Fig. 61: Lab notes - page 2

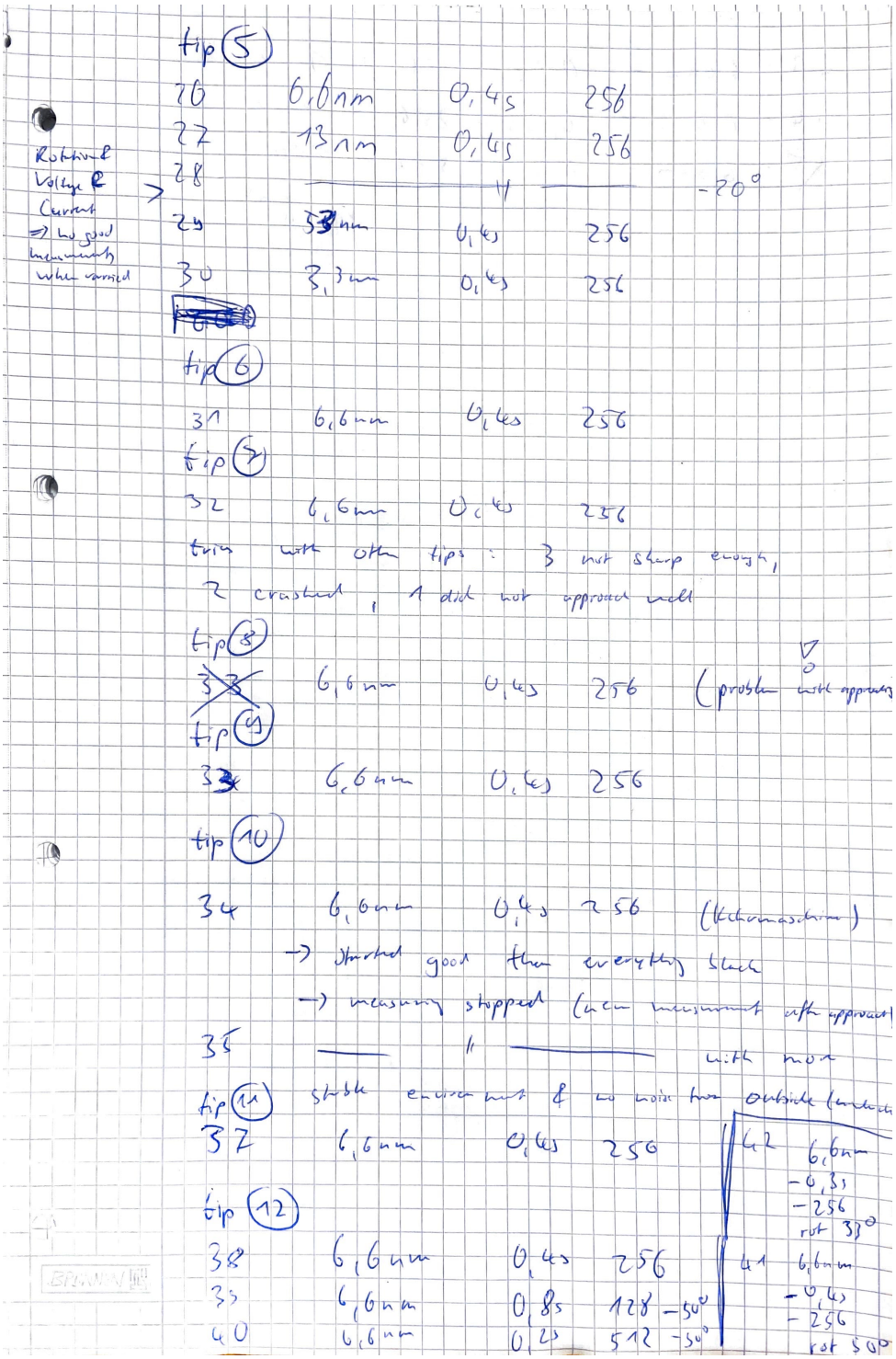

Fig. 62: Lab notes - page 3

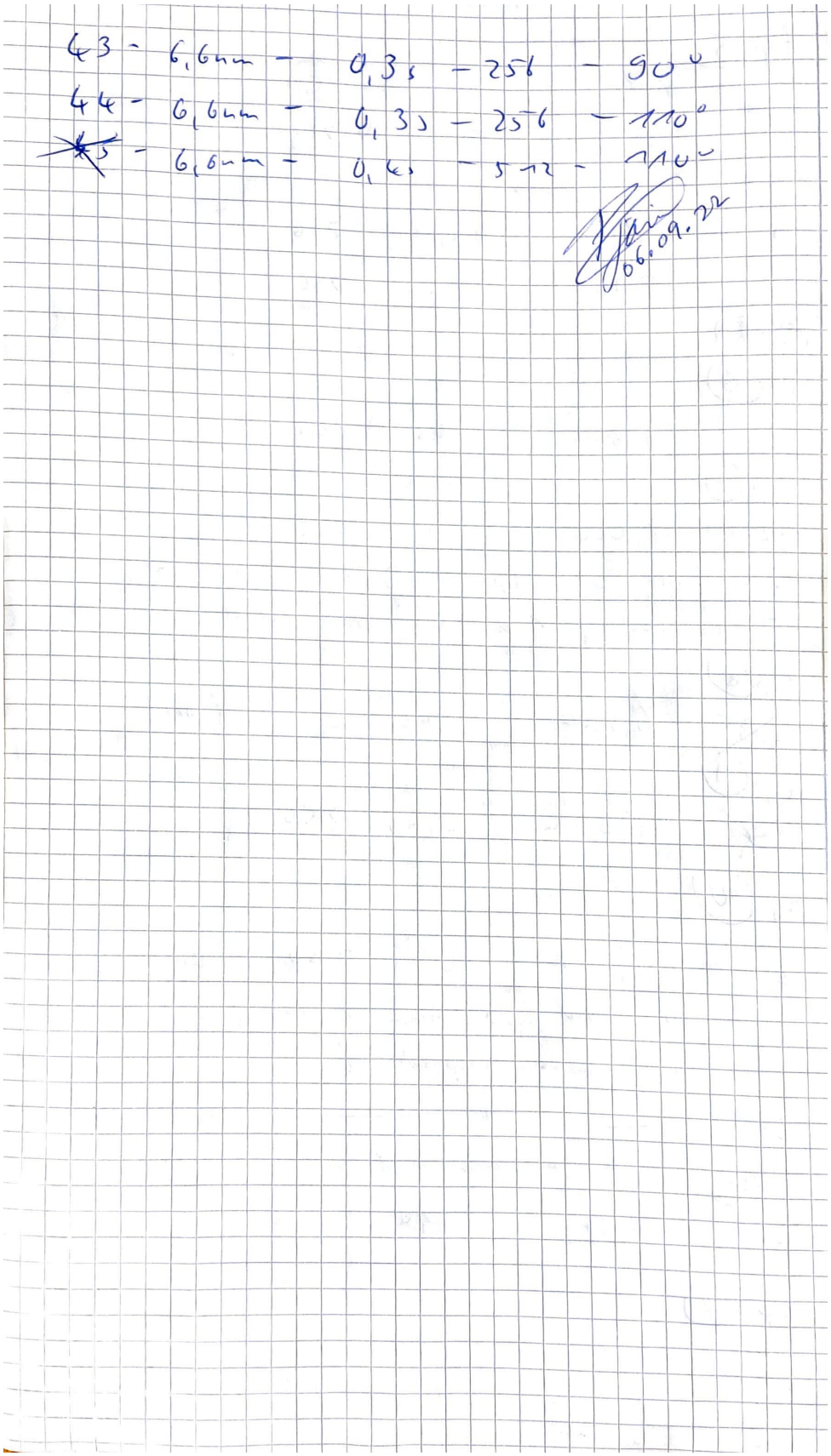

Fig. 63: Lab notes - page 4